



## **An Automated On-line Instrument to Quantify Aerosol-Bound Reactive Oxygen Species (ROS) for Ambient Measurement and Health Relevant Aerosol Studies**

5 Francis P. H. Wragg<sup>1</sup>, Stephen J. Fuller<sup>1</sup>, Ray Freshwater<sup>1</sup>, David C. Green<sup>2</sup>, Frank J. Kelly<sup>2</sup>, Markus Kalberer<sup>1\*</sup>

<sup>1</sup>Department of Chemistry, University of Cambridge, Lensfield Road, CB2 1EW, UK

<sup>2</sup>MRC-PHE Centre for Environment and Health, King's College London, Franklin-Wilkins Building, 150 Stamford Street, London SE1 9NH, UK

10 *Correspondence to:* Markus Kalberer (markus.kalberer@atm.ch.cam.ac.uk)

15

20

25

30

35



## 40 Abstract

The adverse health effects associated with ambient aerosol particles have been well documented, but it is still unclear which aerosol properties are most important for their negative health impact. Some studies suggest the oxidative effects of particle-bound reactive oxygen species (ROS) are potential major contributors to the toxicity of particles. Traditional ROS measurement techniques are labour intense, give poor temporal resolution, and generally have significant delays between aerosol sampling and ROS analysis. However, many oxidizing particle components are reactive and thus potentially short-lived. Thus, a technique to quantify particle-bound ROS online would be beneficial to quantify also the short-lived ROS components.

We introduce a new portable instrument to allow on-line, continuous measurement of particle-bound ROS using a chemical assay of 2',7'-dichlorofluorescein (DCFH) with horseradish peroxidase (HRP), via fluorescence spectroscopy. All components of the new instrument are attached to a containing shell, resulting in a compact system capable of automated continuous field deployment over many hours to days.

From laboratory measurements, the instrument was found to have a detection limit of  $\sim 4$  nmol[H<sub>2</sub>O<sub>2</sub>]equivalents per m<sup>3</sup> air, a dynamic range up to at least  $\sim 2000$  nmol[H<sub>2</sub>O<sub>2</sub>]equivalents per m<sup>3</sup> air, and a time resolution under 12 minutes. The instrument allows for  $\sim 12$  hours automated measurement if unattended, and shows a fast response to changes in concentrations of laboratory-generated oxidised organic aerosol. The instrument was deployed at an urban site in London and particulate ROS levels of up to 24 nmol[H<sub>2</sub>O<sub>2</sub>]equivalents per m<sup>3</sup> air were detected with PM<sub>2.5</sub> concentrations up to 28  $\mu\text{g m}^{-3}$ .

The new and portable On-line Particle-bound ROS Instrument (OPROSI) allows fast-response quantification; this is important due to the potentially short-lived nature of particle-bound ROS as well as fast changing atmospheric conditions, especially in urban environments. The instrument design allows for automated operation and extended field operation. As well as having sensitivity suitable for ambient level measurement, the instrument is also suitable at concentrations such as those required for toxicological studies.

## Keywords

Reactive oxygen species; aerosol; on-line; measurement; health effects; OPROSI; DCFH; HRP.

70

## 1 Introduction

The adverse health effects associated with atmospheric aerosol particles have been well documented in epidemiological studies and further supported with biological cell culture/in-vivo studies; there is a widely accepted association between higher ambient aerosol particle levels and increases in hospital admissions and deaths due to respiratory disease, cardiovascular disease and cancer. (Brunekreef and Holgate, 2002; Dockery et al., 1993; Kunzi et al., 2013; Laden et al., 2006; Lepeule et al., 2012) Due to the large variability in ambient particulate matter, it is still unclear which physical or chemical properties are most important for these negative health effects. Previous studies have suggested particle size, transition metal levels, and elemental carbon levels to be better indicators than simple particle mass concentration.

80



For example, particle size has been strongly correlated to negative health effects due to increased deposition in the alveolar region of the lung, specialised for gas exchange and lacking the cilia-hair clearance system found in the upper respiratory system. Particles with aerodynamic diameter smaller than 2.5  $\mu\text{m}$  ( $\text{PM}_{2.5}$  hereafter) are more likely to deposit in this susceptible lower region of the lung than larger particles are, thus increasing their likely health impact.(Oberdorster et al., 85 2005)

A number of previous studies have highlighted the oxidising capacity of particulate matter as being a potential major cause of their toxicity, particularly with reference to particle-bound or particle-induced reactive oxygen species (ROS), defined here as including families of oxygen-centred or -related free radicals (e.g. HO $\cdot$ , HOO $\cdot$  or ROO $\cdot$ ), ions (e.g. HOO $^-$ ) and molecules (e.g. H $_2$ O $_2$ , organic and inorganic peroxides) with oxidising properties.(Borm et al., 2007; Donaldson et al., 2003; Kramer et al., 2016; MacNee and Donaldson, 2003; Morio et al., 2001; Pryor and Church, 1991; Stevanovic et al., 2013; Wang et al., 2013) It has been argued that deposition of aerosol-bound ROS in the lung, or ROS generation upon deposition in the lung, can lead to a depletion of anti-oxidants naturally present in the lung-lining fluid. This depletion, defined as oxidative stress, can result in an immune response, such as inflammation and proliferation of defence cells. Subsequent cell 95 damage and chronic inflammation may result in increased prevalence of various health issues e.g. Chronic Obstructive Pulmonary Disease, Asthma, and Cardiovascular Disease.(Brunekreef and Holgate, 2002; Dockery et al., 1993; Hart et al., 2015; Lepeule et al., 2012; Oberdorster et al., 2005; Puett et al., 2014)

Whether it be the formation of ROS in situ after particle deposition in the respiratory tract (e.g. through the interaction with transition metal ions and inorganic aerosol) or ROS that are already present on respirable particles to which we are exposed (e.g. organic radicals or peroxides), cell culture studies show there is correlation between the overall oxidative capacity of aerosol particles and their negative effect on human health.(Brunekreef and Holgate, 2002; Steenhof et al., 2011; Tong et al., 2016) 100

Little is known about ROS in the organic fraction of ambient aerosol, despite often making up more than 50 % of submicron aerosol mass.(Jimenez et al., 2009) A potential major contributor to PM-induced health concerns could be water-soluble particle-bound ROS (e.g., peroxides, hydroperoxides, peroxy acids or radicals) in the organic aerosol fraction. A number of studies have attempted to estimate total peroxide content in organic aerosols, leading to the conclusion that peroxides are a significant fraction (10 to >50 %) of aged, oxidized, i.e. atmospherically processed organic aerosol.(Docherty et al., 2005; Hasson and Paulson, 2003; Kramer et al., 2016; Mertes et al., 2012; Vesna et al., 2009; Ziemann, 2005) A main difficulty in analysing organic peroxides and ROS in general in aerosols is the lack of appropriate analytical methods for a reliable quantification. 105 110

It could be argued that the most representative measure of PM-related negative health effects would be via direct in vivo or in vitro exposure. However, these methods are limited by a number of factors including expense, ethics, required measurement timescale, limited suitability for field studies, and often the requirement to collect large amounts of aerosol mass. Alternatively, chemical, acellular, detection methods can provide suitable proxies for the effect of exposure to living tissue. The advantages of such acellular detection methods include reduced labour, increased portability especially for field studies, and more adaptability to target different sources and conditions. Different chemical combinations can focus on 115 different chemical properties potentially linked with the health effects of aerosol. If coupled with biological aerosol exposure methods, this ability to selectively measure specific chemical properties should allow comparisons to overall toxicity to living tissue, ultimately providing information about which chemical properties are most closely linked to aerosol toxicity. 120



125 Traditional off-line acellular aerosol sampling methods for ROS analysis rely on particles being collected on filters or  
impactors, followed by subsequent solvent extraction steps and chemical analysis, and can often take hours to days from  
sample collection to analysis, or substantially longer if storage steps are also considered. But ROS are often not stable or  
long-living (e.g. ROOH, R·, RO<sub>x</sub>· species in particular), so such slow and time-consuming off-line processes may not be best  
suited to determine their atmospheric concentrations, leading to potentially significant underestimates of ROS  
concentrations. This is supported by an earlier study in which we showed ROS concentrations in laboratory-generated  
130 oxidised organic aerosol decreased by a factor of 5–10 within 15 minutes of collection of a sample on a filter, suggesting off-  
line techniques may fail to capture the short-lived, labile, fraction of ROS, instead capturing only the longer-lived, less  
labile, fraction.(Fuller et al., 2014) Further shortfalls of off-line techniques include typical procedures remaining labour- and  
resource-intensive, and the resulting data having poor temporal resolution. Thus, faster, on-line techniques would be more  
suited for reliable quantification of these reactive species.

135

Attempts have been made to create systems with improved temporal resolution relative to off-line filter techniques. Wang *et al.* (2011) and King and Weber (2013) built systems utilising the established fluorescence probe 2',7'-dichlorofluorescein (DCFH) in conjunction with catalytic enzyme horseradish peroxidase (HRP) via fluorescence spectroscopy.(King and Weber, 2013; Wang et al., 2011) The Wang *et al.* (2011) system includes the Particle-into-Liquid-Sampler as a central  
140 component, which relies upon introduction of steam of at least 100 °C. This step could potentially interact with highly  
reactive and labile species, thus potentially introducing artefacts into the ROS measurement.

We further developed the technique by Wang *et al.* (2013) and introduced mild ROS extraction conditions during particle  
collection, thus reducing potential artefacts due to decomposition of labile ROS components at elevated extraction  
145 temperatures.(Fuller et al., 2014) The described system allowed on-line measurement, with a particle collector that allowed  
the sample to be scavenged by the assay within seconds of entering the system, increasing the likelihood of very short-lived  
ROS are also being quantified.

This study describes significant further development and integration of our on-line ROS quantification technique into a  
150 compact and portable on-line ROS instrument capable of automated, continuous, multi-hour, highly time-resolved  
measurement suitable for extended field deployment.

155

## 2 Methods

The new On-line Particle-bound ROS Instrument (OPROSI) comprises four main subunits, as depicted in Fig. 1. The aerosol  
conditioning subunit enables automated blank measurement, removal of particles >2.5 µm, and removal of gases such as  
160 volatile organic compounds and ozone; the particle collection subunit allows collection of particles into liquid phase,  
allowing water-soluble ROS to be extracted; the liquid conditioning subunit provides suitable time and temperature for the  
reaction between the DCFH/HRP assay and extracted ROS components; the detection subunit records fluorescence intensity  
of the assay upon reaction with the sample. A more detailed description of the instrument and its performance is given



165 below, but is preceded by a brief description of the chemical reaction system to quantify ROS (more detail is given in Fuller *et al.* (2014)).

170 The chemical reaction system used to detect ROS is based on the reaction of ROS with horseradish peroxidase (HRP) (Type VI, Sigma Aldrich, 1 Unit ml<sup>-1</sup>, 10% Phosphate Buffer Solution). An aqueous HRP solution is pumped at 1 ml min<sup>-1</sup> into the particle collector (Fig. 1). In the particle collector the HRP solution spray is mixed with the air flow continuously pumped through the particle collector. Water-soluble ROS in aerosol particles are extracted and react with HRP. This particle extract/HRP solution is then combined with an aqueous DCFH solution (10 μM, 10 % PBS), also pumped at 1 ml min<sup>-1</sup>, and the combined mixture passes through a reaction coil for 10 minute where the concentrations of DCFH and HRP are now 5 μM and 0.5 Units ml<sup>-1</sup>, respectively, and where the oxidised HRP reacts with DCFH yielding fluorescent product DCF. The solution is then pumped through the fluorescence spectroscopy continuous-flow cell to quantify the amount of DCF generated, which correlates to the amount of ROS extracted from the aerosol particles.

180 All of the instrument components in Fig. 1 are bolted within or onto a metal shell 60 x 50 x 25 cm in size (adapted from a RS Wall-Mounted Enclosure), with the vacuum pump being the exception to avoid vibrations within the instrument. Figure 2a and 2b show photographs of the instrument, and all components therein. Figure 2a shows the exterior, to which the charcoal denuder, silica gel drier, and mass flow controller are attached. The silver compartment to the right is the liquids enclosure, separating large quantities of liquid from the electronics found inside the main enclosure. This separate compartment also allows chemical containers to be refilled and the waste container to be emptied without needing to open the main enclosure lid, thus reducing disturbance of the instrument's internal conditions during continuous measurement; the chemical containers can be filled from their top-opening and the waste container can be emptied using the waste tap visible in the bottom right of Fig. 2a. The chemical containers connect to the pumps of the liquid system in the main enclosure via quick-release connections, allowing for quick and easy removal for cleaning or refilling. Figure 2b shows the interior of the instrument. Conditions are stable and standardized between different experiments as a result of this enclosed set-up: giving increased temperature stability, better maintained dark conditions and no positional changes of components. Another important benefit of the compact and fixed shell structure is relatively easy movement of the instrument between measurement locations for laboratory or field experiments.

195 Aerosol samples are drawn into the instrument at 5 l min<sup>-1</sup> through the aerosol conditioning unit, which consists first of a stainless steel cyclone (2.5 μm cut-off at 5 l min<sup>-1</sup>, URG-2000-30E-5-2.5-S, URG) thus removing particles > 2.5 μm from the sampled air. The sample then comes to a 3-way solenoid valve (M443W2DFS-LV-132, IPS) which can be controlled to send the sample flow down one of two routes. One route, normally open, leads straight to a custom built activated-charcoal denuder (NORIT® SUPRA pellets, Sigma Aldrich), which removes oxidizing gases, before the flow is then directed to the particle collector. The second route, normally closed, leads to a high efficiency particulate air filter (HEPA CAP 75, Whatman), which removes aerosol particles before re-joining the original route prior to the charcoal denuder. This second route allows for blank measurements to be taken in order to account for fluorescence not due to aerosol-bound ROS. As the solenoid valve can be controlled via LabVIEW, blank measurements can be started and stopped automatically at timed intervals, e.g. during long un-attended experiments, to assess whether the blank/background fluorescence changes with time.

200 After the charcoal denuder the aerosol particles enter the custom built particle collector, described in detail in Fuller *et al.* (2014) and based on designs by Takeuchi *et al.* (2005). (Fuller *et al.*, 2014; Takeuchi *et al.*, 2005) The particle collector



allows extracting water-soluble components of aerosol under mild conditions (i.e. room temperature) and within seconds of entering the particle collector. In the particle collector (PEEK) the aerosol sample flow ( $5 \text{ l min}^{-1}$ ) is combined with the flow of liquid horseradish peroxidase ( $1 \text{ ml min}^{-1}$ ) to form a fine spray of collection solution (Fig. 3). Should water soluble ROS not be extracted at the initial spray-formation stage, they will further come into contact with the HRP solution on the filter stage within the particle collector. This consists of a paper filter (25mm, Whatman Type 1) resting on a PEEK mesh support to assure a constant and uniformly wet filter. From the liquid catchment area, adapted from a glass syringe, the combined HRP and aerosol extract solution is pumped away continuously to be later combined with DCFH. At an air flow rate of  $5 \text{ l min}^{-1}$  and liquid flow rate of  $1 \text{ ml min}^{-1}$ , the particle collector has an efficiency greater than 95 % for aerosol particles  $> 100 \text{ nm}$ , falling to 50 % for  $50 \text{ nm}$  particles.(Fuller et al., 2014) When utilised with the DCFH/HRP assay, collection efficiency this allows a limit of detection of  $4 \text{ nmol}[\text{H}_2\text{O}_2]\text{equivalents per m}^3$  air, which should be suitable for ambient studies at polluted or urban sites.(Fuller et al., 2014; Wang et al., 2011)

For automation of the particle collector sub-unit to be achieved, the liquid height must remain constant in the catchment syringe regardless of potential fluctuation or drift in flows from pumps 1 and 2. This ensures the extracted sample keeps a constant liquid volume, and thus mixing and reaction time, within the catchment syringe. As shown in Fig. 3, adding optical sensors (OPB720, Optek) alongside the catchment syringe, when coupled with a chemically inert reflective floating object at the liquid-air barrier, allows the liquid level height to be detected and subsequently controlled via feedback to pump settings. The device is made from chemically inert Teflon, and is torus-shaped to reduce interference with falling liquid extract drops.

The instrument uses three identical diaphragm pumps (STEPDOS 03, KNF), controlled by a laptop software program (LabVIEW 2013, National Instruments), to pump the HRP solution, the aerosol extract, and the DCFH solution, as indicated in Fig. 1.

After the particle collector, the aerosol extract/HRP solution ( $1 \text{ ml min}^{-1}$ ) is combined with the DCFH solution ( $1 \text{ ml min}^{-1}$ ), as shown in Fig. 1. The liquid flow then enters a thermally stabilised Teflon reaction coil (3.175 mm OD, 1.5 mm ID) where the DCFH reacts with the HRP for 10 minutes in a sealed ethylene glycol bath (heated to  $40 \text{ }^\circ\text{C}$ ), leading to the production of fluorescent dye DCF. The bath is heated using an externally applied heat pad and controlled using a PID controller (Vemer Thermoregulator) and an internal, liquid-resistant, thermistor (NTC liquid probe, 150c, RS). A second thermistor (10K3A1) was placed on the external surface of the bath to track the temperature data. The bath is also surrounded with insulation foam to retain heat and reduce temperature fluctuations.

The solution is then pumped through a custom-built continuous-flow fluorescence spectroscopy cell to quantify the DCF formed in the reaction coil. The flow cell (black acetate) has a vertical flow channel (5 mm diameter, 0.6 ml total volume) where excitation light from a light emitting diode (LED) (470 nm, Luxeon Rebel Star on Coolbase) is delivered via an optical fibre and collimating lens (Ocean Optics) through a quartz rod (25 mm x 3 mm, UQG OPTICS). Fluorescent emission by DCF at 522 nm is transferred via another quartz rod, collimating lens, and optical fibre coupling to an optical spectrometer (Ocean Optics USB2000+; 200-800 nm). The quartz rods act as light channels between the sample flow channel and the collimating lens/optical fibre coupling. The flow channel is vertical at the detection point to allow any potential air bubbles to pass this point as quickly as possible and reduce disturbance of the continuous fluorescence detection.

The LED (470 nm, Luxeon Rebel Star on Coolbase) used for the fluorescence detection was mounted directly onto the cold-plate of a thermo-electric cooler (TECooler) heat-pump assembly (Thermo Electric Devices) to maintain the LED system at



a constant temperature. The cold plate and LED were enclosed in a black acetate enclosure and insulating foam (reducing heat transfer to surroundings). The heat-pump removes excess heat via a fan. This also aids in circulating external air through the instrument, aiding to reduce its internal temperature.

All data obtainment and electronic hardware control is enabled using LabVIEW and a laptop. A multi-channel voltage data logger (1216 series PicoLog, PICO Technologies) is used to collect analogue data from the thermal bath, TECooler, various instrument thermistors, and the syringe optical sensors. It also allows digital control of the solenoid valve and LED driver. All electrical components are powered by USB interface with the laptop, or else via compact and enclosed power supplies (Traco Power TXM Series, TDK Lambda LS Series) fed by one standard mains plug.

### 3 Results

260

#### 3.1 Response of Chemical Assay to Atmospherically-Relevant Compounds

Calibration of the instrument's chemical assay, liquid conditioning and detection systems was achieved using aqueous solutions of known concentrations of ROS model hydrogen peroxide ( $\text{H}_2\text{O}_2$ ). The set-up is adjusted from the Fig. 1 set-up to bypass the aerosol conditioning unit and the particle collector: Teflon tubing connects the HRP bottle directly to pump 2; the DCFH bottle is being replaced by 20 ml vials containing DCFH (same concentration as described before) and  $\text{H}_2\text{O}_2$  (varying concentrations). For  $\text{H}_2\text{O}_2$  calibration, the instrument runs continuously while different  $\text{H}_2\text{O}_2$  concentrations are introduced by switching vials every 10–15 minutes. Figure 4 shows an example of data obtained from such an experiment, with  $\text{H}_2\text{O}_2$  solutions at 0.25–5 mM. Error bars show the standard deviation of multiple measurements ( $n \geq 3$ ). This methodology allows calibration to take place with minimal changes to the fixed instrument, requiring only the addition of a single piece of Teflon tubing, increasing the ease with which calibration can be performed under field measurement conditions.

Using the same method, the DCFH/HRP assay has been tested with, and responded positively to, other water-soluble ROS compounds (organic peroxides and peracids) such as peracetic acid and tert-butylhydroperoxide ( $1.6 \pm 0.2$  and  $16.8 \pm 2.1$  times weaker response than  $\text{H}_2\text{O}_2$ , respectively, for fluorescence intensities equivalent to  $<1 \mu\text{M}$  [ $\text{H}_2\text{O}_2$ ] measured after 10 minute reaction time). The assay showed no response to acetic acid (tested up to  $100 \mu\text{M}$ ), a non-ROS carboxylic acid compound, suggesting similar non-ROS compounds in aerosol particles would not affect the assay's reactivity.

It should be noted that this continuous flow set-up provides an effective time-limit to the reaction; the measured reaction will only occur within the 10-15 minutes before the flow reaches the fluorescence detection point. If the response of the assay to a particular species is too slow, the reaction between them may not reach completion before detection. Using no-flow set-ups, this time was found to be adequate for quick-reacting species such as  $\text{H}_2\text{O}_2$  and peracetic acid. These measurements also show that sterically protected peroxy groups (e.g. in tert-butylhydroperoxide) only react slowly. Therefore, the ROS signal measured in aerosol samples of unknown ROS composition needs to be interpreted as the quantification of the fast-reacting ROS fraction, with slowly-reacting ROS components contributing less to the overall measured ROS concentration.

285



### 290 3.2 Laboratory Measurement of Oxidised Secondary Organic Aerosol

To show the measurement capability of the instrument over a many-hour period, a flow-tube set-up was used to create oxidised secondary organic aerosol (SOA) via ozonolysis of  $\alpha$ -pinene. This is a well-established and reliable method to create SOA with constant concentrations over many hours. (Kroll and Seinfeld, 2008; Lee et al., 2006) A schematic of the set-up used is shown in Fig. 5.

295

Ozone was generated by flowing synthetic air,  $0.2 \text{ l min}^{-1}$ , over an ozone generating ultraviolet (UV) lamp (two lamps were available: one lamp (Pen-Ray 3SC-2, 254 nm) restricted to provide  $\sim 10 \text{ ppm O}_3$ ; and another (SOG1, 184 nm) to provide  $\sim 1 \text{ ppm O}_3$ ). This flow was combined with a flow of  $\alpha$ -pinene-laden nitrogen gas,  $0.2 \text{ l min}^{-1}$ , in a 2 L glass tube, giving a reaction time of  $\sim 5$  minutes, leading to the formation of  $\alpha$ -pinene SOA. The oxidised aerosol was then passed through an activated charcoal denuder to remove excess ozone and organic gaseous species. This was put in place in addition to the permanent denuder of the instrument in order to reduce the possibility of saturation at these unusually high ozone concentrations over many hours. The SOA flow could then be diluted with nitrogen, by a two-stage process, up to a factor of 42 times if required. Particle-bound ROS measurements were performed in parallel with particle size distribution measurements using a Scanning Mobility Particle Sizer (SMPS), allowing comparison between changes in aerosol mass and changes in reported aerosol ROS content. Two different ozone generating UV lamps were used in the same experiment in an attempt to achieve a greater range of aerosol concentrations, from very high masses ( $\sim 740\text{--}180 \mu\text{g m}^{-3}$  via the Pen-Ray 3SC-2) to lower masses ( $\leq 110 \mu\text{g m}^{-3}$  via the SOG-1).

300

305

The fluorescent spectrometer recorded an average of 100 spectra (200-800 nm) every 1.0-1.5 seconds. The SMPS recorded scans every 3 minutes, and comprised a TSI model 3081 differential mobility analyser (DMA) and a 3776 condensation particle counter (CPC), set to a sampling rate of  $3.0 \text{ L min}^{-1}$  and a DMA sheath flow of  $0.3 \text{ l min}^{-1}$ . Particle number size distribution data (14-670 nm) was obtained using TSI AIM software, and converted to particle mass concentration using  $1 \text{ g cm}^{-3}$  as the assumed density of the oxidised aerosol.

310

Figure 6 shows data from such an  $\alpha$ -pinene ozonolysis experiment, demonstrating operation over  $\sim 12$  hours and with varying aerosol concentrations. The dotted red line shows the SOA mass concentration values obtained by the SMPS. The black line shows fluorescence intensity due to ROS components in the extracted aerosol sample. The first  $\sim 6$  hours of the experiment shows how the instrument responds to changing total aerosol mass concentration. Reducing the aerosol mass concentration by dilution, leads to a reduced fluorescence reading, as shown in the first 5 hours of the experiment shown in Fig. 6.

320

The final  $\sim 5$  hours of the experiment in Fig. 6 shows the performance of the instrument stability and the automated blank measurement system. The shaded areas in this period correspond to times when the HEPA filter was put in-line in the aerosol conditioning unit, described above and shown in Fig. 1. During these periods, any aerosol, and thus any aerosol-bound ROS, are removed from the sample after entering the instrument, reducing the fluorescence reading to blank levels.

This automated process of switching between sample measurement and blank measurement gave repeatable values. When measuring aerosol-bound ROS for long periods of time, occasional periods with the HEPA filter in-line should be taken to follow trends in blank measurement values. Potential discrepancy between different blank measurement periods could derive from e.g. a drifting of assay reactivity over time, or from charcoal denuder efficiency lessening over time.

325





330 Raw fluorescence data can then be blank subtracted and converted from fluorescence units (counts) into ROS concentration units (nmol[H<sub>2</sub>O<sub>2</sub>]equivalents per m<sup>3</sup> air) using the H<sub>2</sub>O<sub>2</sub> calibration curve (Fig. 4), gas flow rate at the particle collector, and liquid flow rate at the detection point, via Eq. (1).

$$\text{ROS Conc (nmol[H}_2\text{O}_2\text{]equiv./ m}^3\text{ air)} = \frac{\text{ROS Conc (nmol[H}_2\text{O}_2\text{]equiv./ L)} \times \text{Liquid Flow Rate (L / min)}}{\text{Gas Flow Rate (m}^3\text{ / min)}} \quad (1)$$

335

Approximately 3 hours into the experiment, the O<sub>3</sub>-generating UV lamp was replaced by a less powerful lamp to allow generation of a wider range of SOA concentrations. Due to the fact that the two lamps provided different [ROS] per [aerosol] ratios, the fluorescence reading after the changeover point remained approximately constant despite the aerosol mass concentration dropping from ~200 to ~100 µg m<sup>-3</sup>. While it is not entirely clear what causes this difference in [ROS] per [aerosol] ratio, it could be explained by the different aerosol concentrations in the flow tube, as generated by the two lamps: at higher aerosol concentrations (e.g. due to the more powerful lamp), more high-volatility compounds (e.g. aldehydes) will be incorporated into the particles, thus reducing the fraction of the particle mass that is composed of ROS such as peroxides and peroxy-acids. With lower aerosol concentrations in the flow tube (due to the less powerful lamp), the high-volatility compounds are less likely to be incorporated in the particle mass, but the less volatile ROS species will still be present in the particle mass, leading to a higher [ROS] per [aerosol] ratio. The particles were only diluted a few seconds before collection in the ROS instrument, which might not have been sufficient to allow particle components to reach thermodynamic equilibrium.

340

345

Figure 7 shows ROS concentration, in nmol[H<sub>2</sub>O<sub>2</sub>]equivalents per m<sup>3</sup> air, plotted against SMPS aerosol mass concentration for the experiment described above. The black circles represent data taken when the more powerful UV lamp was used, and the blue diamonds represent data when the less powerful UV lamp was used. The [ROS] per [aerosol] produced with the two lamps is different, but in both cases positive linear correlations are observed. Note that the Fig. 7 does not include data for the periods of transition between the different concentration plateaus.

350

The time it took for the OPROSI reading to transit from one concentration plateau to another was approximately 12 minutes, regardless of whether the change was due to transition between two different sample concentrations, or due to transition between blank and sample measurements (through introduction of the HEPA filter). Thus, 12 minutes could be considered a suitable value for OPROSI time resolution for use with cases of instantaneous changes of 10–425 µg m<sup>-3</sup> oxidised SOA, as per the experiment shown in Fig. 6. However, changes of this magnitude are unlikely to occur so rapidly in ambient conditions, so the OPROSI time resolution may be lower in value when atmospherically relevant concentration changes are considered. Even the conservative time resolution value of 12 minutes should be sufficient to resolve most expected ROS concentration changes in the ambient atmosphere.

355

360

### 3.3 Ambient Measurement of Particle-Bound ROS at an Urban Roadside Site using the OPROSI

Fig. 8 shows an example of ROS data during a winter-time ambient measurement campaign at a Department of Environment Food and Rural Affairs (Defra) Automatic Urban and Rural Network (AURN) roadside measurement site on Marylebone Road, London, UK. Measurements were taken via a 360° inlet, ~1 metre away from, and ~4 metres above, the edge of the roadside. PM<sub>2.5</sub> levels were recorded by Defra using a Filter Dynamics Measurement System Tapered Element Oscillating Microbalance (FDMS-TEOM).

370



The gaps in the data shown in Fig. 8 correspond to periods when extended blank measurements were taken. Data from this campaign show that our new instrument is sensitive enough to detect changes in ambient ROS levels at a polluted urban site in the UK and can measure over a period of 24 hours with minimal user interaction (as discussed above). ROS concentrations of 4–24 nmol[H<sub>2</sub>O<sub>2</sub>]equivalents per m<sup>3</sup> air were measured during a ~24 hour period with PM<sub>2.5</sub> concentrations of 5–28 µg m<sup>-3</sup>, and a range of 0.4–2.7 nmol[H<sub>2</sub>O<sub>2</sub>]equivalents per µg[PM<sub>2.5</sub>]. When comparing this AURN PM<sub>2.5</sub> data to the ROS data, there does appear to be some potential correlation of their general trends throughout the 24 hour period. Further measurements will be undertaken during periods of higher photochemistry, e.g. summer-time, to see what affect this has on the correlation between ROS measurements and PM<sub>2.5</sub> data.

Our recorded ROS concentration of 4–24 nmol[H<sub>2</sub>O<sub>2</sub>]equivalents per m<sup>3</sup> air is comparable in magnitude to that found by Wang *et al.* during their 2011 study in Rochester, New York, USA, in which they stated an average ROS concentration of  $8.3 \pm 2.19$  nmol[H<sub>2</sub>O<sub>2</sub>]equivalents per m<sup>3</sup> air over a period of seven days. King and Weber (2013), however, mentioned a number of measurements below their limit of detection, and stated an average ROS concentration of 0.26 nmol[H<sub>2</sub>O<sub>2</sub>]equivalents per m<sup>3</sup> air for their urban site in Atlanta, USA. At present it is difficult to determine whether these ROS concentration differences are due to the location studied, sample studied, or due to differences in instrument design.

#### 4 Conclusions

A compact instrument, OPROSI, has been designed and built to be capable of continuous automated and unattended quantification of particle-bound reactive oxygen species (ROS) over many hours using the HRP/DCFH assay. It is contained within a metal shell for ease of transportation and field measurement deployment. The OPROSI was designed with a view to making the instrument automated for long periods of time, but also to detect changes over a timescale of minutes and will therefore be suitable for health-related air pollution studies as well as for atmospheric process studies. The instrument uses mild aerosol extraction conditions that should reduce measurement artefacts due to decomposition of labile ROS components. It has a detection limit of 4 nmol[H<sub>2</sub>O<sub>2</sub>]equivalent per m<sup>3</sup> air and a time resolution estimate of ~12 minutes with laboratory-generated oxidised aerosol. The OPROSI has shown capability of several days successful continual functionality with minimal user interference (e.g. refilling liquid bottles and emptying waste bottle), and ~12 hours with no user interference required.

The new instrument was tested with laboratory-generated oxidised-SOA via  $\alpha$ -pinene ozonolysis and showed clear correlation between ROS intensity and oxidised-SOA mass. Ambient measurements were taken at an urban site in London, UK, which showed the OPROSI is sensitive enough for ambient ROS measurement.

#### 405 Data Availability

Data can be made available upon requests to the corresponding author.

#### Author Contributions

MK conceived the study and oversaw research. SJF developed the initial technique. FPHW designed and developed the instrument, designed and performed the experiments, analysed the data, and wrote the manuscript. RF designed and built many of the electronic components required to run the instrument. DG and FK facilitated access to the Marylebone Road site in London and provided the PM<sub>2.5</sub> data. All authors have read and approved the final manuscript.



### Acknowledgements

415 The authors would like to thank ERC (the European Research Council, grant 279405) for their funding of this study. Infrastructure at Marylebone Road was supported by NERC (the Natural Environment Research Council, Clearflo grant NE/H003231/1) and Defra (Department of Environment Food and Rural Affairs, contract AQ0643 Automatic London Network (2010-14) RMP 5442). Thanks also to Keith Gray, Richard Nightingale, and colleagues for their help with various custom-built components and incorporation into the final instrument structure.

420

### References

- Borm, P.J.A., Kelly, F., Kunzli, N., Schins, R.P.F., Donaldson, K., Oxidant generation by particulate matter: from biologically effective dose to a promising, novel metric, *Occupational and Environmental Medicine* 64(2007), pp. 73-74.
- 425 Brunekreef, B., Holgate, S.T., Air pollution and health, *Lancet* 360(2002), pp. 1233-1242.
- Docherty, K.S., Wu, W., Lim, Y.B., Ziemann, P.J., Contributions of organic peroxides to secondary aerosol formed from reactions of monoterpenes with O<sub>3</sub>, *Environmental Science & Technology* 39(2005), pp. 4049-4059.
- 430 Dockery, D.W. *et al.*, An Association Between Air-Pollution and Mortality in 6-United-States Cities, *New England Journal of Medicine* 329(1993), pp. 1753-1759.
- Donaldson, K. *et al.*, Oxidative stress and calcium signaling in the adverse effects of environmental particles (PM<sub>10</sub>), *Free Radical Biology and Medicine* 34(2003), pp. 1369-1382.
- Fuller, S.J., Wragg, F.P.H., Nutter, J., Kalberer, M., Comparison of on-line and off-line methods to quantify reactive oxygen species (ROS) in atmospheric aerosols, *Atmospheric Environment* 92(2014), pp. 97-103.
- 435 Hart, J.E. *et al.*, The association of long-term exposure to PM<sub>2.5</sub> on all-cause mortality in the Nurses' Health Study and the impact of measurement-error correction, *Environmental Health* 14(2015), p. 9.
- Hasson, A.S., Paulson, S.E., An investigation of the relationship between gas-phase and aerosol-borne hydroperoxides in urban air, *Journal of Aerosol Science* 34(2003), pp. 459-468.
- 440 Jimenez, J.L. *et al.*, Evolution of Organic Aerosols in the Atmosphere, *Science* 326(2009), pp. 1525-1529.
- King, L.E., Weber, R.J., Development and testing of an online method to measure ambient fine particulate reactive oxygen species (ROS) based on the 2',7'-dichlorofluorescein (DCFH) assay, *Atmospheric Measurement Techniques* 6(2013), pp. 1647-1658.
- Kramer, A.J. *et al.*, Assessing the oxidative potential of isoprene-derived epoxides and secondary organic aerosol, *Atmospheric Environment* 130(2016), pp. 211-218.
- 445 Kroll, J.H., Seinfeld, J.H., Chemistry of secondary organic aerosol: Formation and evolution of low-volatility organics in the atmosphere, *Atmospheric Environment* 42(2008), pp. 3593-3624.
- Kunzi, L. *et al.*, Responses of lung cells to realistic exposure of primary and aged carbonaceous aerosols, *Atmospheric Environment* 68(2013), pp. 143-150.



- 450 Laden, F., Schwartz, J., Speizer, F.E., Dockery, D.W., Reduction in fine particulate air pollution and mortality -  
Extended follow-up of the Harvard six cities study, *American Journal of Respiratory and Critical Care  
Medicine* **173**(2006), pp. 667-672.
- Lee, A. *et al.*, Gas-phase products and secondary aerosol yields from the ozonolysis of ten different terpenes,  
*Journal of Geophysical Research-Atmospheres* **111**(2006), p. 18.
- 455 Lepeule, J., Laden, F., Dockery, D., Schwartz, J., Chronic Exposure to Fine Particles and Mortality: An Extended  
Follow-up of the Harvard Six Cities Study from 1974 to 2009, *Environmental Health Perspectives*  
**120**(2012), pp. 965-970.
- MacNee, W., Donaldson, K., Mechanism of lung injury caused by PM10 and ultrafine particles with special  
reference to COPD, *European Respiratory Journal* **21**(2003), pp. 47S-51S.
- 460 Mertes, P., Pfaffenberger, L., Dommen, J., Kalberer, M., Baltensperger, U., Development of a sensitive long path  
absorption photometer to quantify peroxides in aerosol particles (Peroxide-LOPAP), *Atmospheric  
Measurement Techniques* **5**(2012), pp. 2339-2348.
- Morio, L.A. *et al.*, Tissue injury following inhalation of fine particulate matter and hydrogen peroxide is  
associated with altered production of inflammatory mediators and antioxidants by alveolar macrophages,  
465 *Toxicology and Applied Pharmacology* **177**(2001), pp. 188-199.
- Oberdorster, G., Oberdorster, E., Oberdorster, J., Nanotoxicology: An emerging discipline evolving from studies  
of ultrafine particles, *Environmental Health Perspectives* **113**(2005), pp. 823-839.
- Pryor, W.A., Church, D.F., Aldehydes, Hydrogen-Peroxide, and Organic Radicals as Mediators of Ozone  
Toxicity, *Free Radical Biology and Medicine* **11**(1991), pp. 41-46.
- 470 Puett, R.C. *et al.*, Particulate Matter Air Pollution Exposure, Distance to Road, and Incident Lung Cancer in the  
Nurses' Health Study Cohort, *Environmental Health Perspectives* **122**(2014), pp. 926-932.
- Steenhof, M. *et al.*, In vitro toxicity of particulate matter (PM) collected at different sites in the Netherlands is  
associated with PM composition, size fraction and oxidative potential - the RAPTES project, *Particle  
and Fibre Toxicology* **8**(2011), p. 15.
- 475 Stevanovic, S. *et al.*, Influence of Oxygenated Organic Aerosols (OOAs) on the Oxidative Potential of Diesel and  
Biodiesel Particulate Matter, *Environmental Science & Technology* **47**(2013), pp. 7655-7662.
- Takeuchi, M., Ullah, S.M.R., Dasgupta, P.K., Collins, D.R., Williams, A., Continuous collection of soluble  
atmospheric particles with a wetted hydrophilic filter, *Analytical Chemistry* **77**(2005), pp. 8031-8040.
- Tong, H. *et al.*, Hydroxyl radicals from secondary organic aerosol decomposition in water, *Atmos. Chem. Phys.*  
480 **16**(2016), pp. 1761-1771.
- Vesna, O., Sax, M., Kalberer, M., Gaschen, A., Ammann, M., Product study of oleic acid ozonolysis as function  
of humidity, *Atmospheric Environment* **43**(2009), pp. 3662-3669.
- Wang, D.B. *et al.*, Macrophage reactive oxygen species activity of water-soluble and water-insoluble fractions of  
ambient coarse, PM2.5 and ultrafine particulate matter (PM) in Los Angeles, *Atmospheric Environment*  
485 **77**(2013), pp. 301-310.

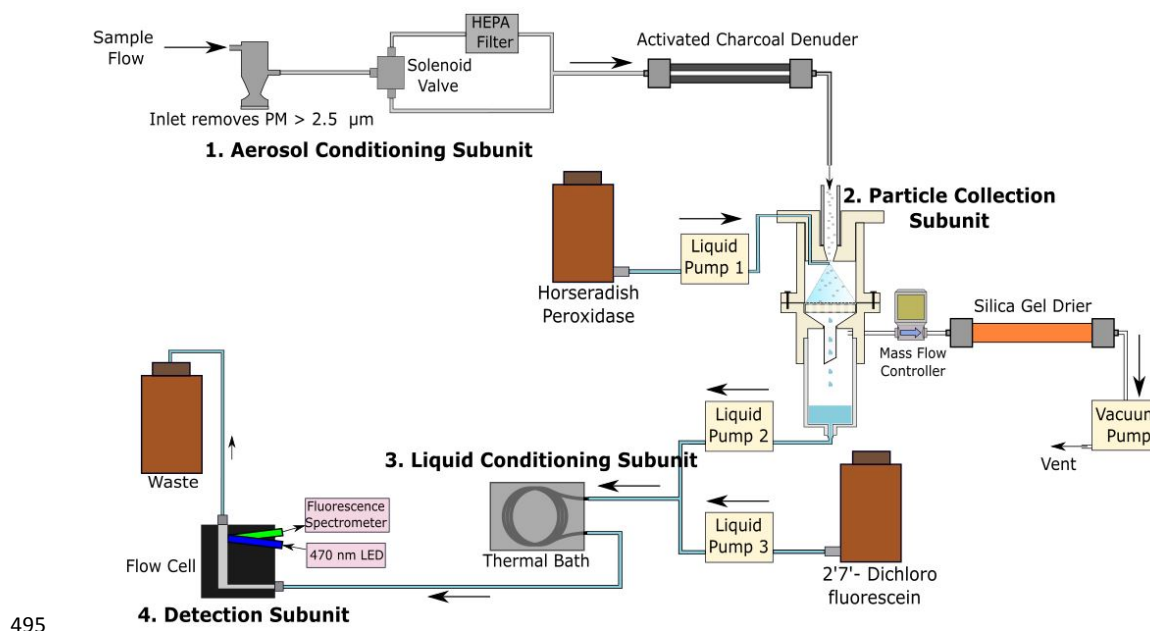


Wang, Y., Hopke, P.K., Sun, L., Chalupa, D.C., Utell, M.J., Laboratory and field testing of an automated atmospheric particle-bound reactive oxygen species sampling-analysis system, *Journal of toxicology* **2011**(2011), p. 419476.

490 Ziemann, P.J., Aerosol products, mechanisms, and kinetics of heterogeneous reactions of ozone with oleic acid in pure and mixed particles, *Faraday Discussions* **130**(2005), pp. 469-490.



## Figures and Figure Captions



495

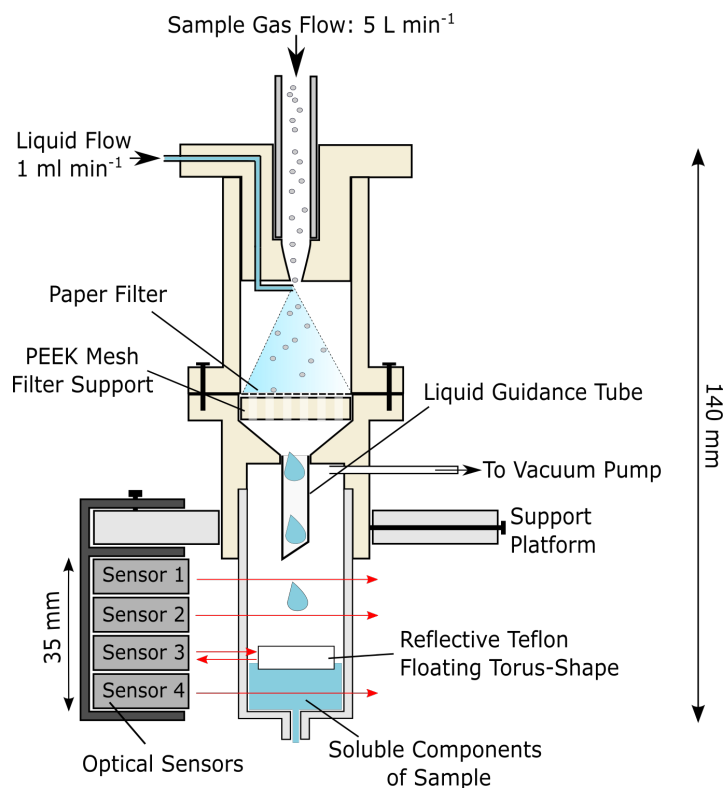
**Figure 1.** Schematic diagram of the new portable On-line Particle-bound ROS Instrument (OPROSI), comprising four labelled subunits. (1) the aerosol conditioning subunit enables removal of particles  $>2.5 \mu\text{m}$ , automated blank measurement, and removal of gases such as volatile organic compounds and ozone; (2) the particle collection subunit allows collection of particles into liquid phase, allowing soluble ROS to be extracted; (3) the liquid conditioning subunit provides suitable time and temperature for the reaction between the DCFH/HRP assay and extracted ROS components; (4) the detection subunit records fluorescence intensity of the assay upon reaction with the sample.

505

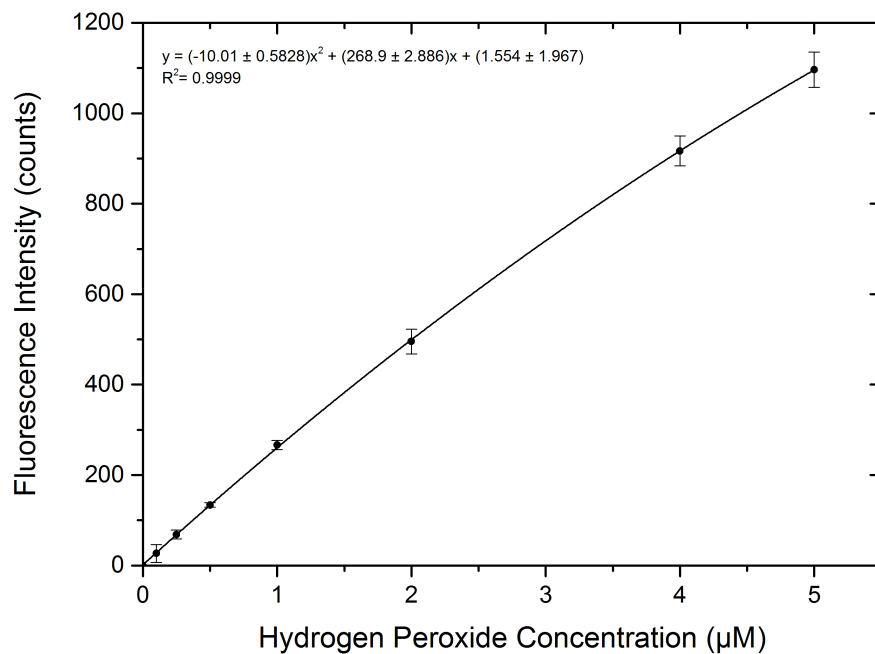


**Figure 2.** The exterior (2a) and interior (2b) of the new and portable Online Particle-bound ROS Instrument (OPROSI). All components shown are attached and integrated into, or onto, a portable box (60 x 50 x 25 cm) to allow easier deployment for field studies.

510



515 **Figure 3.** Schematic diagram of the particle collector allowing collection of particle-bound, water-soluble ROS components under mild extraction conditions. Addition of the reflective optical sensor system allows liquid height to be detected and subsequently controlled, thus allowing automated measurement for extended periods of time under constant reaction conditions.



520

**Figure 4.** Example of a calibration of the on-line instrument using standard ROS compound hydrogen peroxide ( $\text{H}_2\text{O}_2$ ) in the concentration range of 0.25–5  $\mu\text{M}$ .

525

530



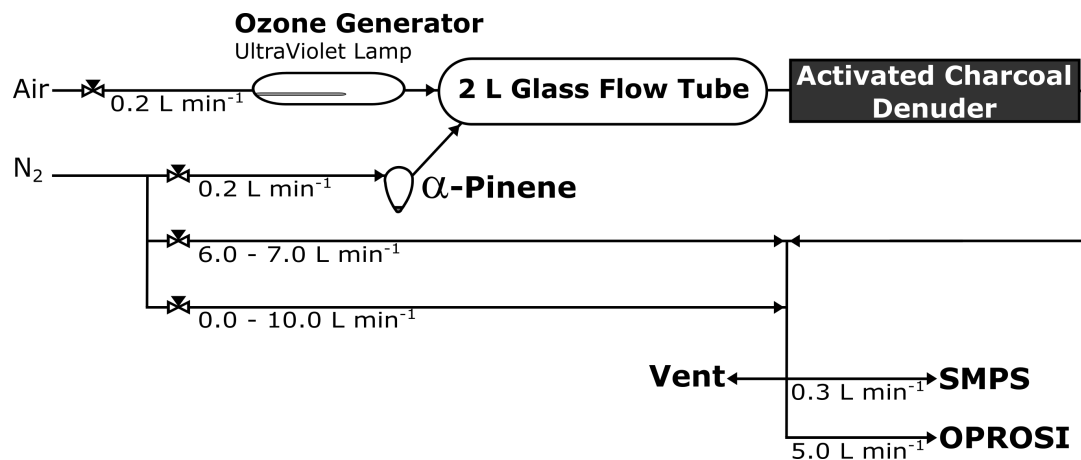
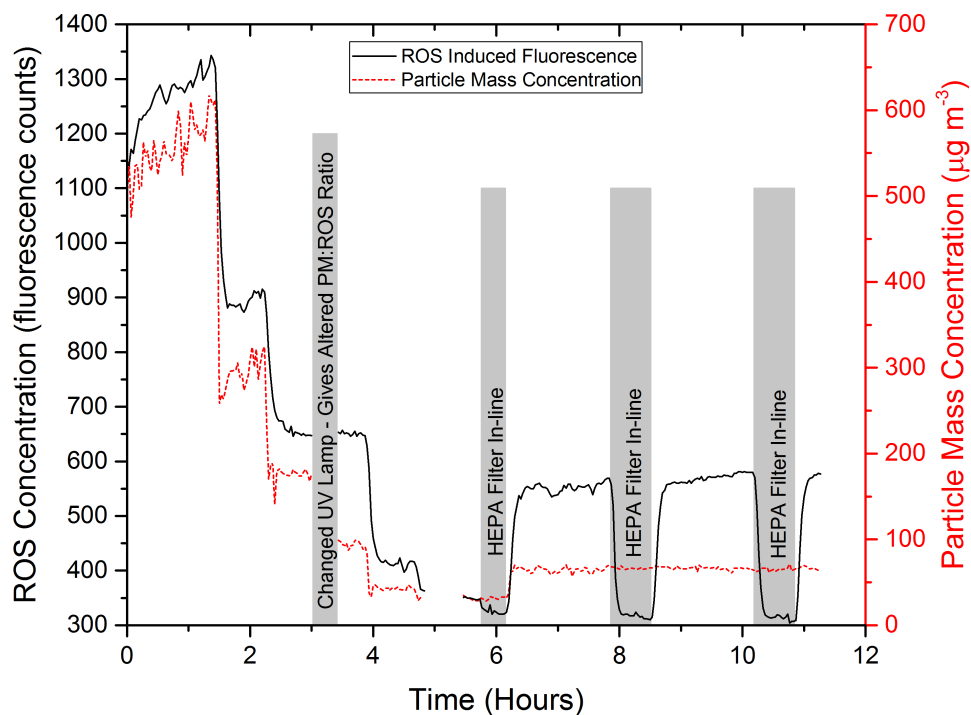


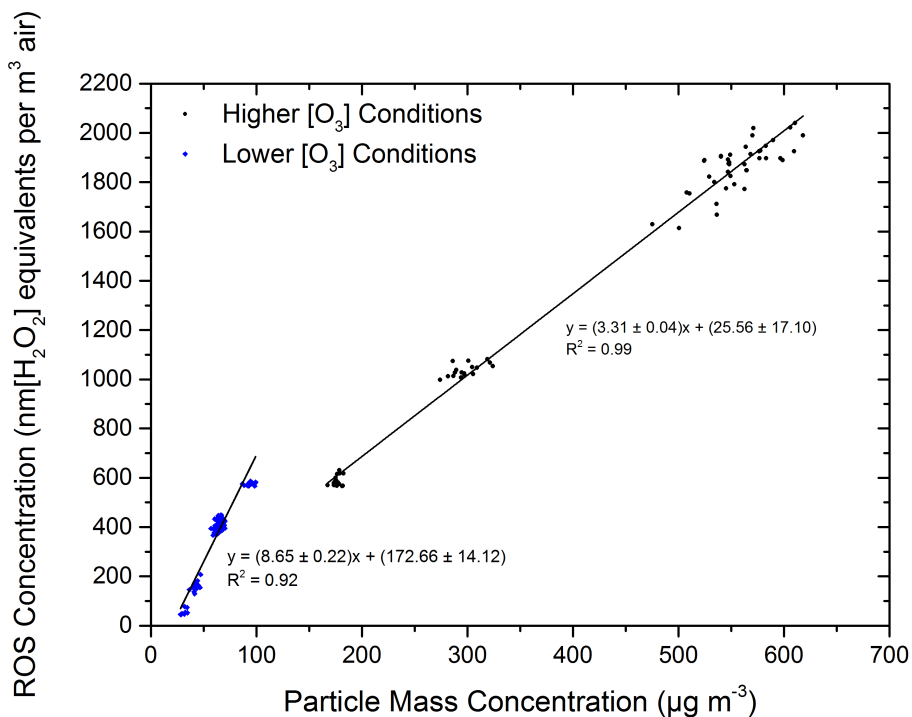
**Figure 5.** Experimental set-up to produce and measure varying concentrations of oxidised secondary organic aerosol (SOA) via ozonolysis of  $\alpha$ -pinene. Ozone generating lamps of two different strengths were used to generate two different  $\alpha$ -pinene SOA concentrations in the flow tube, which, when combined with subsequent optional dilution up to a factor of 42, enabled a wide range of aerosol masses to be measured.



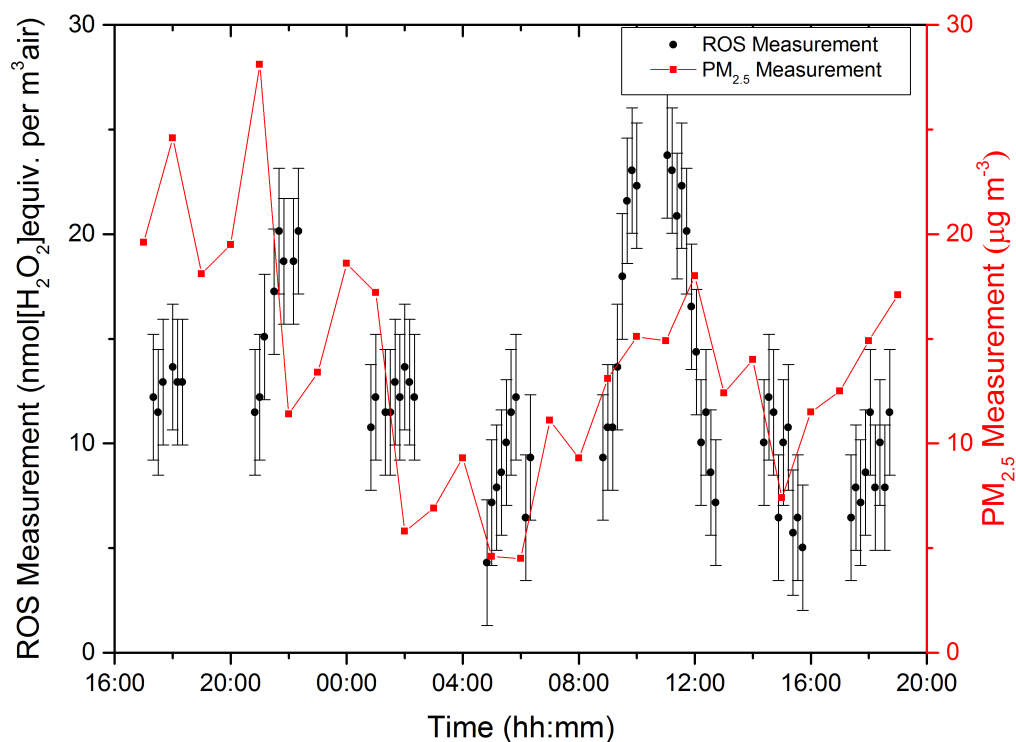
540

**Figure 6.** Data from  $\alpha$ -pinene ozonolysis SOA laboratory experiment, showing the OPROSI response to changes in mass concentration of oxidised aerosol in addition to the effect of the automated blank measurement system and the long-term stability of the instrument.

545



550 **Figure 7.** ROS concentration (OPROSI) vs mass concentration of  $\alpha$ -pinene SOA particles (SMPS). The two different flow tube/ozone lamp conditions, provided SOA with different ROS content, confirmed by the different linear correlations shown between aerosol mass and ROS concentration.



555

**Figure 8.** A ~24 hour time series of ambient ROS measurement from an urban roadside site in central London, UK (Marylebone Road). Black circles represent 10 minute averages of OPROSI data ( $\text{nmol}[\text{H}_2\text{O}_2]\text{equiv. per m}^3\text{ air}$ ). Red squares show hourly averages of  $\text{PM}_{2.5}$  ( $\mu\text{g m}^{-3}$ ).